HIGH SPATIAL RESOLUTION MEASUREMENTS USING HYDROGEOPHYSICAL METHODS REVEAL THE PRESENCE OF HOTSPOTS FOR BIOGENIC GAS ACCUMULATION AND RELEASE IN THE FLORIDA EVERGLADES

by

Troy Bole

A Thesis Submitted to the Faculty of

Charles E. Schmidt College of Science

In Partial Fulfilment of the Requirements for the Degree of

Master of Science

Florida Atlantic University

Boca Raton, FL

May 2019

HIGH SPATIAL RESOLUTION MEASUREMENTS USING HYDROGEOPHYSICAL METHODS REVEAL THE PRESENCE OF HOTSPOTS FOR BIOGENIC GAS ACCUMULATION AND RELEASE IN THE FLORIDA EVERGLADES

by

Troy Bole

This thesis was prepared under the direction of the candidate's thesis advisor, Dr. Xavier Comas, Department of Geosciences, and has been approved by all members of the supervisory committee. It was submitted to the faculty of the Charles E. Schmidt College of Science and was accepted in partial fulfillment of the requirements for the degree of Master of Science.

SUPERVISORY COMMITTEE:

Xavier Comas, Ph.D.
Thesis Advisor

Tara Root, Ph.D.

Brian Benscoter, Ph.D.

Zhixiao Xie, Ph.D.
Chair, Department of Geosciences

Ata Sarajedini, Ph.D.
Dean, Charles E. Schmidt College of Science

Khaled Sobhan, Ph.D.
Interim Dean, Graduate College

4-8-2019
Date

ACKNOWLEDGEMENTS

I would like to thank my advisor, Dr. Xavier Comas for his endless support and guidance during both the field aspect and writing of this manuscript. I would also like to thank my committee members: Dr. Tara Root and Dr. Brian Benscoter for their constructive review of this research and thesis. This work was partially supported by National Oceanic and Atmospheric Administration, NOAA (GC11-337); and U.S. Geological Survey, under the Greater Everglades Priority Ecosystems Science. I would like to thank MALA Geosciences for help with equipment support and particularly to Amber Onufer and Phil Oviatt. I thank all those that helped with the field work and data acquisition including Matthew Sirianni, Matthew McClellan, Thomas Shahan, Joe Becker, Michael Rebar, Aaron Duecaster, Jake Stefanick, Eric Miller, James Anthony and many others.

ABSTRACT

Author: Troy A. Bole

Title: High spatial resolution measurements using hydrogeophysical methods reveal the presence of hotspots for biogenic gas accumulation and release in the Florida Everglades

Institution: Florida Atlantic University

Thesis Advisor: Dr. Xavier Comas

Degree: Master of Science

Year: 2019

It is well known that biogenic gas emissions (mainly methane and carbon dioxide) vary both spatially and temporally in peatlands. While most studies have focused on northern systems, several recent studies in tropical and subtropical peatlands (like the Everglades) have revealed the presence of areas of increased gas accumulation and emissions, or hotspots, that may be related to physical and/or biogeochemical changes within the peat's matrix. However, these studies are often limited in terms of sampling volume and resolution or are based in laboratory studies that may not be totally representative of field conditions. In this study we investigate the spatial variability (both lateral and vertical) in gas accumulation and release at the field scale, over 10 m long transects at two locations in Water Conservation Area 1 of the Florida Everglades, using an array of hydrogeophysical methods. Resulting data infers the presence of hotspots with dimensions ranging from 1-2 m in width and approximately 0.5 m tall. These areas showed high variations in biogenic gas accumulation and release an order of magnitude

higher than surrounding areas and occur seasonally as the highest gas releases were observed during Florida’s wet season. This study therefore has implications for better understanding the spatial and temporal variability of biogenic gas hotspots in peat soils, and how the matrix structure affects gas accumulation and release. This study shows the importance of considering the heterogenous nature of the peat's matrix when quantifying gas fluxes in the Everglades, and particularly when using methods with small sampling volumes like gas chambers.

HIGH SPATIAL RESOLUTION MEASUREMENTS USING HYDROGEOPHYSICAL METHODS REVEAL THE PRESENCE OF HOTSPOTS FOR BIOGENIC GAS ACCUMULATION AND RELEASE IN THE FLORIDA EVERGLADES

LIST OF FIGURES

LIST OF TABLES

LIST OF EQUATIONS

1 INTRODUCTION

Peatlands are known to store a substantial amount of carbon (C) (as much as 688 Gt), while only covering approximately 3% of the Earth's surface [Yu et al., 2010]. Peatlands can sequester atmospheric C for thousands of years and are the largest terrestrial storage of organic C [Parish et al., 2008]. Tropical peatlands store approximately 15-30% of the global carbon pool and comprise 18-25% of the global volume of peatlands [Limpens et al., 2008; Page et al 2011]. Although most studies on peatlands have traditionally focused on boreal systems, studies on tropical and subtropical peatlands have increased in the last two decades. Some of these recent studies have focused on improving quantification of C stocks in tropical and subtropical systems [McClellan et al, 2016; Comas et al, 2017; Saragi-Sasmito et al., 2018] but also in better understanding patterns of variability in the production, accumulation and release of biogenic gases from peat soils [Shoemaker et al., 2015; Wright et al, 2016].

Peatlands are one of the largest natural sources of CH_4 (methane), a greenhouse gas with a global warming potential over twenty-eight times greater than CO_2 (carbon dioxide) [Myhre et al., 2013]. Free-phase CH_4 in peatlands is formed through methanogenesis by methanotrophic archaea, which induce two different process: the splitting of acetate and the reduction of CO_2 with H_2 [Conrad, 1999; Whalen, 2005]. Biogenic CH_4 accumulates within the peat matrix as a free-phase gas, travels upward to the peat surface, and over time, moves through the soil via diffusion or is released into the atmosphere through the process of ebullition and wicking through vascular plants

[Joabsson et al., 1999]. While most studies investigating gas dynamics in peat soils have traditionally focused on boreal systems, many recent studies have emphasized investigating gas dynamics in subtropical systems like the Everglades. Table 1 shows a compilation of some of these studies depicting estimates of accumulated biogenic gas content, gas flux released, and inferred gas production from a variety of peat soils located in Florida, using a wide range of methodologies, and consequently, also a wide range in spatial and temporal scales of measurement. These studies highlight the large variability in estimates (exceeding between 2-3 orders of magnitude), ranging between 1.9-21% gas content, 2.2-852.8 mg CH_4 m^{-2} d^{-1} in gas releases, or 8.0-641.8 mg CH_4 m^{-2} d^{-1} in gas production. Furthermore, while some of these studies have stressed spatial variability, such variability relies on average estimates in gas content and fluxes per site, comparing differences between sites spread across several miles. For example, Wright and Comas [2016] showed spatial variability in gas dynamics for several sites in Water Conservation Area (WCA) 2 and 3 but did not explore spatial variability in gas accumulation and release for specific sites. One of the few studies investigating smaller trends in spatial variability is Mustassar and Comas (2017), which included descriptions of hotspots for gas accumulation and release in a peat monolith from the Everglades at the laboratory scale. Other recent studies have used computational models to understand the nature of these hotspots in the Everglades [Wright et al, 2018].

Table 1. Summary of previous data sources showing gas content, release and production in both lab and field settings using various methodologies.

Study	**Study site**	**Methods**	**Average gas content in soil (%)**	**Average gas release (CH_4 m^{-2} d^{-1}) (mg)**	**Average gas build-up (production) (CH_4 m^{-2} d^{-1}) (mg)**

Chanton et al., 1988	Everglades, multiple locations	Gas bubble collection	ND	5.6	ND
Comas & Wright, 2012	Everglades, WCA-1	Gas traps, time-lapse camera	ND	3-68	ND
Comas & Wright, 2014	Everglades, WCA-1	GPR, gas traps, time-lapse camera	2.1-16.9	33.8-132.3	8-25 mg
Comas & Wright, 2014	Everglades, WCA-3	GPR, gas traps, time-lapse camera	1.9-13.5	71.6-718.8	315.6-641.8 mg
Shoemaker et al., 2015	Everglades, Dwarf Cypress	Eddy covariance	ND	19-36	ND
Wright & Comas, 2016	Everglades, WCA-2	GPR, gas traps, time-lapse camera	9-17	90-200	180-290 mg
Wright & Comas, 2016	Everglades, WCA-3	GPR, gas traps, time-lapse camera	6-12	60-250	180-310 mg
Li & Mitsch, 2016	Corkscrew Swamp, Florida	Gas storage containers	ND	2.2-53.4	ND
Mustasaar & Comas, 2017	Everglades, LILA	GPR, gas traps, surface deformation	4-12	33.3-852.8	ND
Wright et al., 2018	Everglades, WCA-3	MEGA (computer model)	8-21	ND	ND

Note. ND = no data.

The presence of hotspots for biogenic gas production, accumulation and release has been described in boreal peatlands in several studies and has traditionally been attributed to differences in microhabitat [Waddington et al, 1996; Baird et al, 2004; Green and Baird, 2013]. Some studies have attributed the presence of areas of increased

biogenic gas accumulation to changes in the physical properties of the peat matrix, including the presence of wood layers, that may act as confining layers for the accumulation of biogenic gas within the peat matrix [Comas et al, 2005; Parsekian et al, 2011; Comas et al, 2013], however these studies do not necessarily relate increased gas accumulation to enhanced gas production. In subtropical peatlands, the presence of hotspots has also been accredited to physical and structural changes of the peat matrix, which may be related to differences in humification (and therefore biogeochemical properties), and consequently determines biogenic gas production and ebullition patterns [Mustasaar and Comas, 2017; Wright et al, 2018]. Temporal variability in gas accumulation and release has also been largely investigated over the last 2-3 decades and has often been associated with environmental factors such as fluctuations in water table elevation, and periods of both increased and decreased atmospheric pressure [Bon et al., 2014; Chen & Slater, 2015; Comas et al., 2011; Glaser et al., 2004; Wright and Comas, 2016].

Furthermore, studies show a large variability in terms of hotspot dimensions. In a study investigating carbon fluxes in Finland using high resolution aerial images, Becker et al. [2008] concluded that ground resolutions of 25-60 cm would be sufficient for detecting biogeochemical hotspots for CH_4 and CO_2 flux emissions. Other studies have shown hotspots for gas accumulation ranging between 5 m wide, 2 m thick, and extending laterally as much as 100 m [Comas et al., 2005; Parsekian et al., 2011]. At the laboratory scale and for Everglades soils, Mustassar and Comas [2017] described hotspots ranging between 5 and 10 cm in diameter. From all these studies, it seems clear that our knowledge on the spatial and temporal distribution of hotspots for biogenic gas

accumulation and release in peat soils is still incomplete, particularly for subtropical peatlands and for studies based on field scales rather than laboratory incubations.

In this paper, we explore the presence of hotspots for gas accumulation and release in subtropical peat soils of the Everglades at the field scale. Both spatial and temporal variability in biogenic gas content accumulation and release is estimated using time-lapse GPR measurements at two sites in the Loxahatchee National Wildlife Refuge in the Water Conservation Area 1 (WCA-1) of the Everglades (FL). The study combines measurements to explore both lateral variability (cm scales) in gas dynamics for 10 m long transects and variability with depth (m scales) to infer the presence of hotspots. This work has implications for better understanding the role of peatlands as a major greenhouse gas contributor under a changing climate scenario.

2 STUDY SITES

Peat soil has been accumulating in the Everglades for approximately 4,000 years and reaches thicknesses of more than 3 m in some areas [Glaser et al., 2012; Gleason and Stone, 1994]. In the mid-1900's, a system of water storage areas was created to meet the increasing water demand from agriculture and growing population in South Florida. These storage areas are named water conservation areas, WCA-1, 2 and 3, each hydrologically separated from the other. WCA-1 (also known as The Loxahatchee National Wildlife Refuge) is a wetland with over 140,000 acres of swamp located in the northernmost portion of the Florida Everglades, and contains the deepest peat deposits. WCA-1 contains mostly Loxahatchee peat and contains some of the highest organic content (92%) in the Everglades [Craft and Richardson, 2008]. The area is predominantly lily pads (Nymphaea odorata), sawgrass (Cladium jamaicense) and tree islands that form a ridge and slough topography that provide habitat to a large variety of wildlife [Craft and Richardson, 2008; Davis and Ogden, 1994]. The sloughs provide an excellent setting for GPR transects and other methods for sampling biogenic gases because they are inundated for nearly the entire year. Sampling locations for this project were determined using large scale GPR transects in areas where the peat-clay boundary was easily visible. Two study

sites (Site E and Site W) were chosen from these large scale transects (Figure 1).

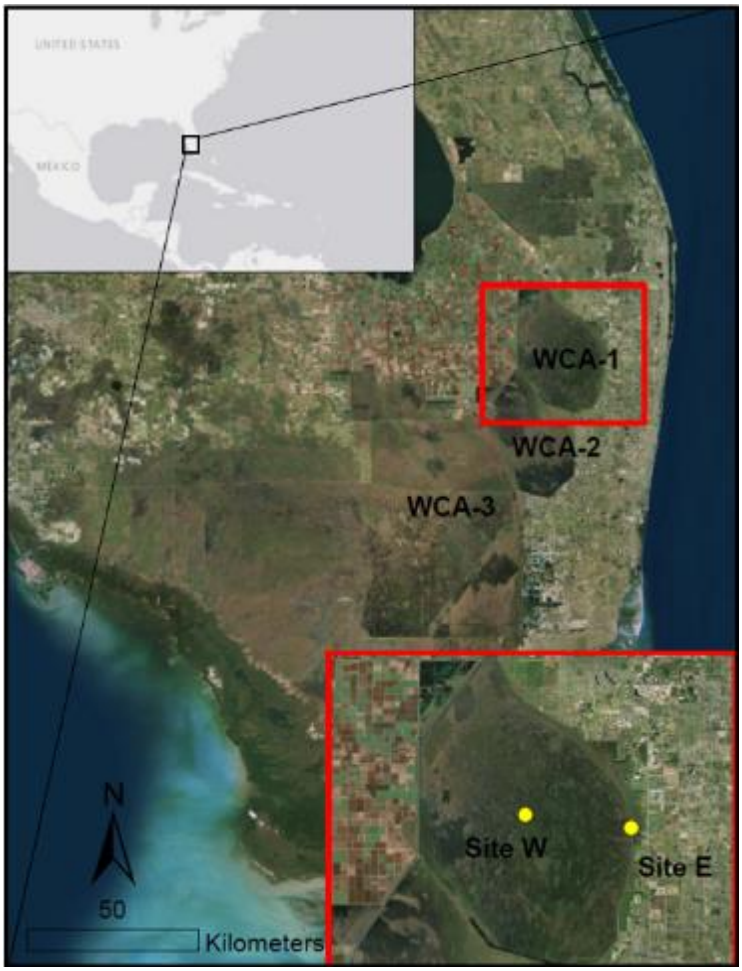

Figure 1. Satellite image showing location of study sites in WCA-1 in the Florida Everglades: Site W and Site E (yellow dots).

3 METHODOLOGY AND EXPERIMENTAL SETUP

GPR is a non-invasive hydrogeophysical method with an antenna that transmits high-frequency electromagnetic (EM) waves that are reflected and returned to a receiver. Common offset mode (transmitter and receiver maintain the same separation as they move along a transect) was used for all surveys in this study [Neal, 2004]. At both sites, a 10 m long wooden platform attached to wooden pilings fixed to the mineral soil was built to allow for a repeatable transect without disturbing the peat matrix and/or gas regime (Figure 2). An array of Mala RAMAC shielded antennas with frequencies of 160, 450 and 750 MHz was initially used to survey the study sites. Time-lapse measurements however were performed only with the 160 MHz antenna since it provided the best depth of penetration to reach the mineral soil interface. All data collected were processed using ReflexW software by Sandmeier Scientific. The following common filters were applied to the data: dewow (to eliminate low frequency noise), manual y-gain (to enhance deeper signals and normalize amplitudes), background removal (high-pass filter), static correction (to eliminate time delay) and bandpass (to eliminate high and low-frequency noise).

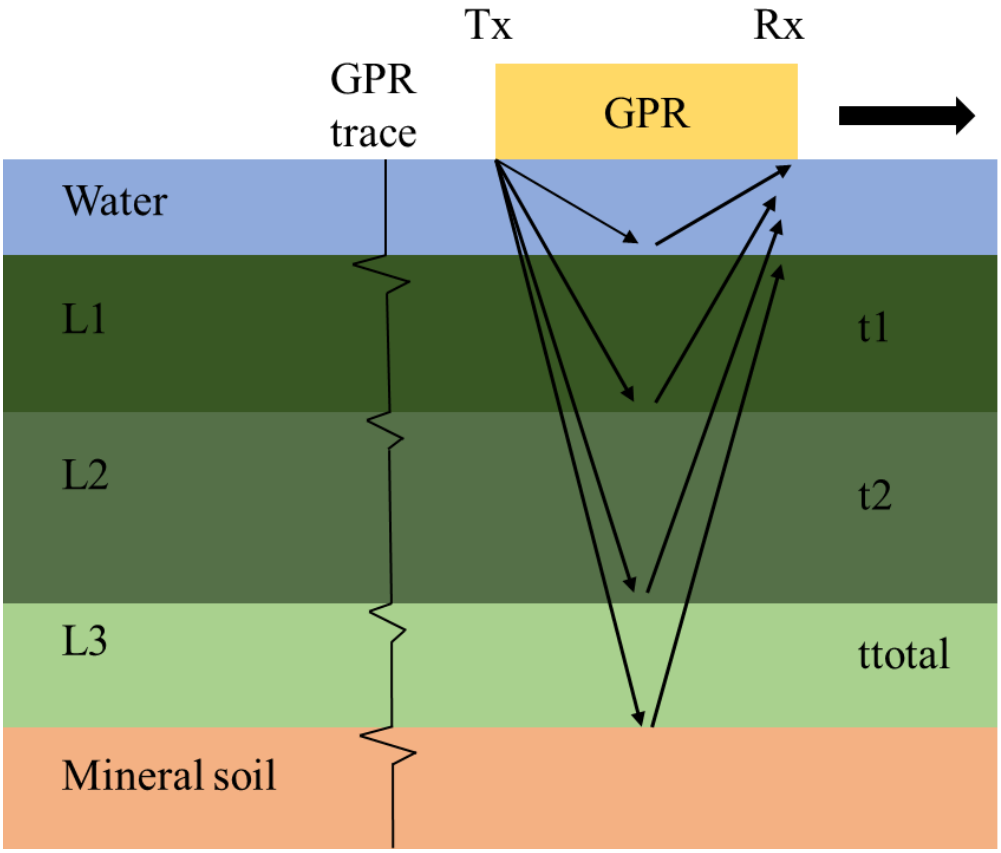

Figure 2. Conceptual diagram exemplifying a GPR survey at Site W. Interfaces within the peat matrix allow to infer a total of three layers (L1-L3), and the EM wave travel time associated to each interface (t1, t2 and ttotal). Also, a simplified trace highlighting each interface is shown in the center.

At both sites, reflectors were manually picked that represented the following stratigraphic interfaces: (1) the water column-peat surface interface; (2) marked interfaces within the peat layer representative of changes in physical properties (i.e. humification), as confirmed from coring (one for Site E and two for the Site W); and (3) the peat-mineral soil interface (Figure 2). The same reflectors were picked over time, representing a set of 188 laterally spaced traces or vertical travel time values (in ns) across the 10 m platform with specific values for each dataset. A total of 17 transects were collected at each site between October 10, 2016 and October 13, 2018. While initially a spacing of 2-

3 weeks was intended between datasets, field conditions (i.e. weather, water table elevation, etc.) and equipment availability dictated data acquisition. A set of 10 cores (spaced about 1 meter) was collected ((offset from the GPR transect as to not disturb the sampling line) at each platform to record lateral changes in peat thickness across the platform. Using these values and interpolating in between cores, travel times for each trace were converted to EM wave velocity (v), and the relative dielectric permittivity calculated as defined by:

$$v = \frac{Co}{\sqrt{\varepsilon_r(b)}}$$

(Equation 1)

where Co is the speed of light (3 x 10^8 ms^{-1}) and ε_r is the bulk relative dielectric permittivity of the soil. The value of ε_r is highly dependent on water content, and sites were permanently fully indundated during our measurements, so we consider that changes ε_r are due to changes in gas content.

Finally, the Complex Refractive Index Model (CRIM) was used [Huisman et al., 2003] to calculate gas content from the ε_r estimate at each trace and for each dataset. The CRIM is a volumetric three-phase mixing model for soils and is defined as:

$$\varepsilon_r{}^{\alpha}{}_{(b)} = \theta\varepsilon_r{}^{\alpha}{}_{(w)} + (1-n)\varepsilon_r{}^{\alpha}{}_{(s)} + (n-\theta)\varepsilon_r{}^{\alpha}{}_{(\alpha)}$$

(Equation 2)

where $\varepsilon_{r(b)}$ is the bulk relative dielectric permittivity (= 1), $\varepsilon_{r(w)}$ is relative dielectric permittivity of the water (temperature dependent), $\varepsilon_{r(s)}$ is the relative dielectric permittivity of the soil (constant value of 2 based on Comas and Slater [2004]), n is the total porosity, θ is the volumetric soil water content, and α is an exponential factor using

the orientation of the electrical field of minerals (a constant value of 0.35 typically used for peat soils based on Comas et al [2005] and Kellner and Lundin [2001]). In this equation, gas content is represented by $(n - \theta)$. Gas content in this study was expressed as either: a) a percent gas content value per trace and for each layer within the two platforms, i.e. two layers at Site E and three at Site W; and b) a two-dimensional (2D) plot based on the interpolation of the gas content values above using the kriging method.

Changes in gas content can also be used to estimate gas flux values of CH_4 per day by using gas composition from onsite gas traps (as explained later) and expressed as mg CH_4 m^{-2} d^{-1}. In this case, however it is critical to have a good understanding of the sampling volume inferred in our GPR measurement. Using the concept of the first Fresnel Zone of GPR, volume can be approximated by the ellipsoid volume [Červený and Soares, 1992] as:

$$v = \frac{4}{3}\pi abc$$

(Equation 3)

where a, b, and c are the semiaxes of the ellipsoid defined as

$$a = \frac{1}{2}\left(\frac{\lambda}{4} + L\right)$$

(Equation 4)

$$b, c = \frac{1}{2}\left(\frac{\lambda^2}{4} + L\lambda\right)^{1/2}$$

(Equation 5)

where λ represents wavelength (is calculated using the antenna frequency) and L is the length the ray traces along its path. An additional array of methods was also used to

constrain the GPR measurements. Gas traps were used to measure gas ebullition (or the amount of gas released into the atmosphere from the peat) infer rates of gas release, and to capture gas to determine carbon composition of the gas (i.e. CH_4 and CO_2) using gas chromatography. Each site contained two gas traps attached to the platform to collect and analyze gas. Trap design followed Wright et al, 2018, and consisted of a 3.9 cm clear 1-inch PVC graduated cylinder attached at one end by a fitted valve for sampling, and the other by an inverted PVC funnel (with a diameter of 20 cm). The funnels were placed a few cm above the top of the peat (above the flocculant layer) and submerged below the water surface. During sampling, all gas was removed from the chamber and water was pulled into the chamber using a syringe. The total volume of gas removed was collected during each visit and the gas analyzed in the field using a LandTec GEM2000 portable gas analyzer for percentages of CH_4 and CO_2.

Capacitance moisture probes were also installed at each site and used to measure water temperature within the peat soil. The Decagon 5TE probes are 10 cm x 3.2 cm x 0.7 cm with a sampling volume of 0.2 dm^{-1}. The capacitance probes were placed approximately 20-30 cm below the surface of the peat.

A Russian peat corer was used to extract cores from both sites to measure depth of peat, humification and porosity. The corer has a semicylindrical head and rotating cutting edge that removes a core 50 cm long with minimal disturbance of the peat matrix. The corer was used to extract samples for porosity values at each 50 cm depth as well as determining the total thickness of the peat from the water column to the mineral soil. In the field, a von Post humification scale was used to determine the decomposition of the peat from a scale of H1 (undecomposed peat) to H10 (highly decomposed peat) [Verry et

al. 2011]. This subjective analysis of humification of peat is done on the same day by the same person to reduce human error. Cores were taken back to the lab and used to measure porosity. Average porosity (two for each layer) was determined by saturating and weighing a sample with a known volume then drying it for 48 hours at 105°C according to ASTM standards [American Society for Testing and Materials A. S. T. M., 2014].

4 RESULTS

4.1 PHYSICAL PROPERTIES

Peat thickness, humification and porosity values with depth are shown in Figures 3a and 3b for Site E and Site W respectively. Lateral peat thickness ranges between 1.84-1.99 m for Site E and between 2.80-3.00 m for Site W as based on the coring performed. Based on the von Post humification and the porosity measurements, two peat layers were inferred for Site E (Figure 3a): layer one (L1E) with a thickness of 0.85 m, humification of H1/2, and porosity of 95.1%; and layer two (L2E) with a thickness of 1.05 m, humification of H4/5, and 94.7% porosity. Using the same approach, three peat layers were inferred at Site W, (Figure 3b): layer one (L1W), with a thickness of 0.85 m, humification of H1/2, and porosity of 97.1%; layer two (L2W), with a thickness of 1.25 m, humification of H3/4 and porosity of 96.4%; and layer three (L3W), with a thickness of 0.85 m, humification of H3/4, and porosity of 93.4%.

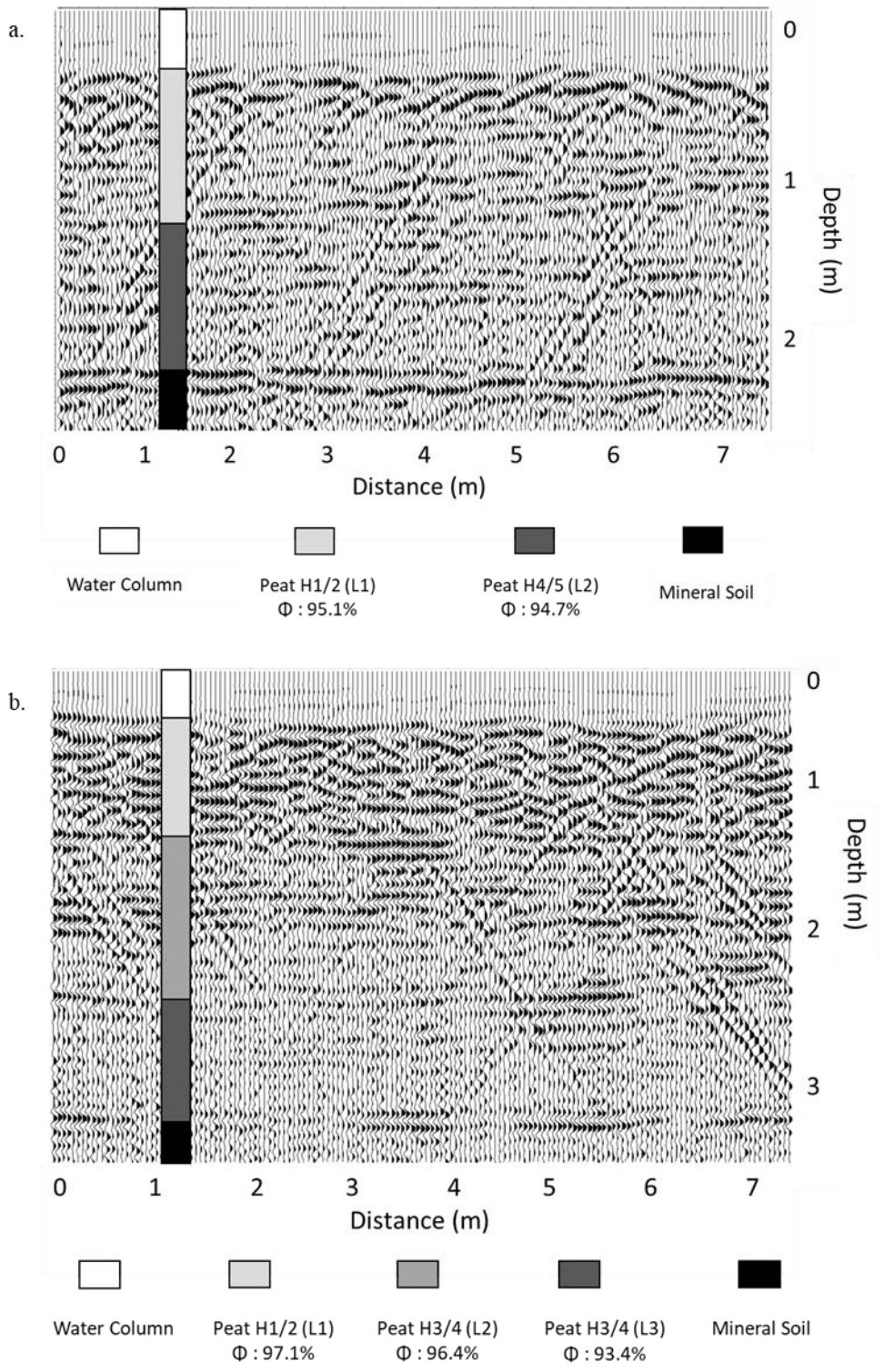

Figure 3. Processed GPR profile of Site E (a) and Site W (b) with corresponding humification and porosity values for each layer.

4.2 GPR DATA

4.2.1 COMMON OFFSET PROFILES

Discrete common offset GPR profiles with a length of approximately 7.5 m are shown for both Site E and Site W taken on October 13, 2018 (Figure 3a and 3b). While only the profiles for this specific date are shown, they are representative for the time-lapse series, and show some characteristic features that match the coring results. First, the contrasts in von Post humification from the cores coincide well with laterally continuous reflectors that support the inferred layer distribution at each site (i.e. two vs. three layers for Site E and Site W respectively). Secondly, such layer distribution is also supported by some changes in the appearance of the reflector record (commonly referred as radar facies, i.e. Neal, 2004). For example, layer 1 at Site W (Figure 3b) is characterized by a discontinuous and chaotic configuration of reflectors that contrasts with a more horizontal and continuous distribution for layer 2 and 3, and a layer 3 showing an increased attenuation that also contrasts with a sharp peat-mineral soil interface below. A similar reflector record can also be interpreted for Site E (Figure 3a). In both cases common offsets also show a series of diffraction hyperbolas coinciding with the position of the platform legs.

4.2.2 TIME-LAPSE SERIES

The GPR common offset time-lapse series was used to infer the spatial and temporal distribution of gas content along each platform using Equation 2 (details in the methodology section above). Gas content at each platform was expressed both as an overall average for the entire peat column, and as a series of vertically stacked layers. Gas content distribution across each platform is shown in Figure 4a and 4b for Site E and

Site W respectively. Results for Site E (Figure 4a) show an overall average with gas content values reaching up to 16.1% and overall averages of 6.5% (Table 2). When considering gas content per layer, the shallowest layer L1E shows a range in gas contents up to 28.0% and an overall average of 8.8%, underlain by a second layer L2E with gas contents up to 17.5%, and an overall average of 5.3%. Results for Site W show an overall average of 4.0% with gas contents reaching values up to 12.6%. The shallowest layer at Site W, L1W reaches values up to 26.2% and an overall average of 8.6%. The middle layer, L2W has gas content reaching 18.4% and an overall average 8.2%, underlain by the deepest layer, L3W with values up to 24.0% and an overall average of 6.6%. As shown in Figure 4a, maximum variability along the platform is found between 2.1 and 3.9 m and within layer L1E, while the least variability is found along the platform between 0 and 1.5 m, and between 4.3 and 7.3 m and within layer L2E. As shown in Figure 4b, maximum variability along the transect is found between 1.3 and 4.3 m and within layer L1W, while the least variability is found between 4.5 and 6.6 m and within layer L2W. In both cases, the deepest layer shows the least average gas content.

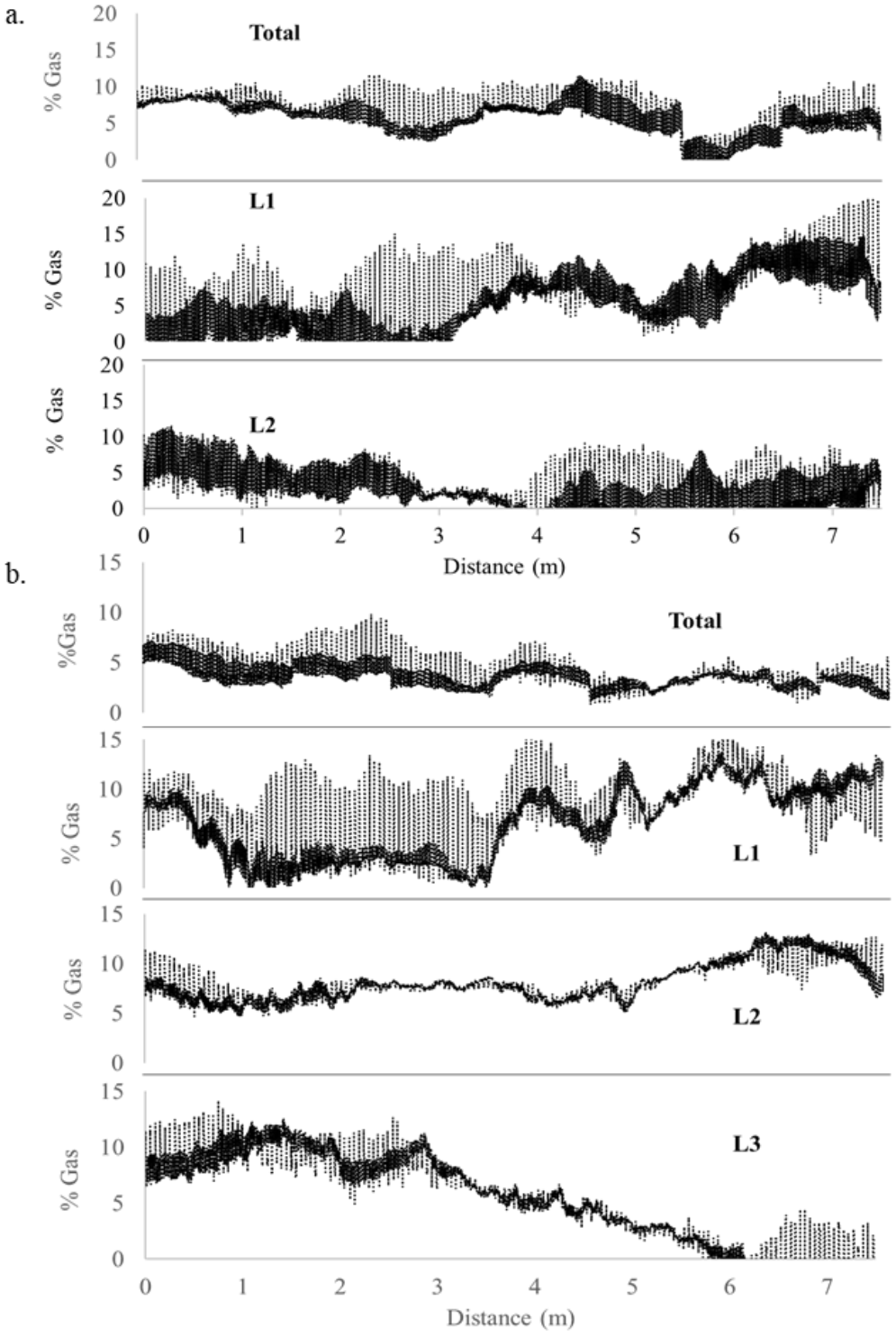

Figure 4. Gas content for total peat and each peat layer at Site E (a) and Site W (b).

Table 2. Gas content for each peat layer from Site E and Site W using GPR.

Layer	Depth (m)	Thickness (m)	Avg. Von Post	Avg. Porosity (%)	Average (% gas)	Max (% gas)
L1E	0 – 0.85	0.85	H1/2	95.1	8.8	28.0
L2E	0.85 – 1.9	1.05	H4/5	94.7	5.3	17.5
E Avg.	0 – 1.9	1.9	H3	94.9	6.5	16.1
L1W	0 – 0.85	0.85	H1/2	97.1	8.6	26.2
L2W	0.85 – 2.1	1.25	H3/4	96.4	8.2	18.4
L3W	2.1 – 2.95	0.85	H3/4	93.4	6.6	24.0
W Avg.	0 – 2.95	2.95	H3	95.6	4.0	12.6

Two-dimensional (2D) plots of gas content considering average values per layer and for specific survey times are shown in Figure 5. It is important to consider that either 2 or 3 gas content values with depth for each trace (as inferred from the interpreted layers at Site E and Site W respectively) are considered here when inferring 2D distribution of gas content at each platform, and that the rest of the values are interpolated using the kriging method. As shown in Figure 5a, Site E is characterized by some specific areas that consistently show progressive increases and decreases in gas content from March 22 to October 13, 2018. For example, Figure 5a shows an area (see box on Figure 5a) of approximately 2 m (between 2-4 m along the transect) by 1 m (entire peat column) that ranges from 0 to 17.7% gas content with an average of 7.2% for March 22, a range of 0 to 24.2% with an average of 10.5% for April 2, a range of 0 to 28.0% with an average of 9.3% for June 20, and a range of 0.2 to 21.7% with an average of 7.2 for October 13. Within this area, pockets of about 1 m by 0.5 m (like that between 2-3 m along the transect and 0-0.5 m depth) show progressive increases in gas content followed by a decrease that represents changes of more than 25% gas content. Similarly, Site W is also characterized by specific areas that consistently show progressive increases and decreases

in gas content from March 8 to June 20, 2018. Figure 5b shows an area (see box in Figure 5b) of approximately 3 m by 2 m with a range of 0.1 to 19.7% gas content and an average of 7.7% for March 8, a range of 0.4 to 21.4% with an average of 8.6% for March 22, a range of 0.0 to 25.9% with an average of 10.1% for April 18, and a range of 0.0 to 19.2% with an average of 6.8% for June 20. Once again, and within this area, pockets of about 1-2 m by 0.5 m show a progressive gas content build-up followed by a decrease also representing more than 25% decrease in gas content.

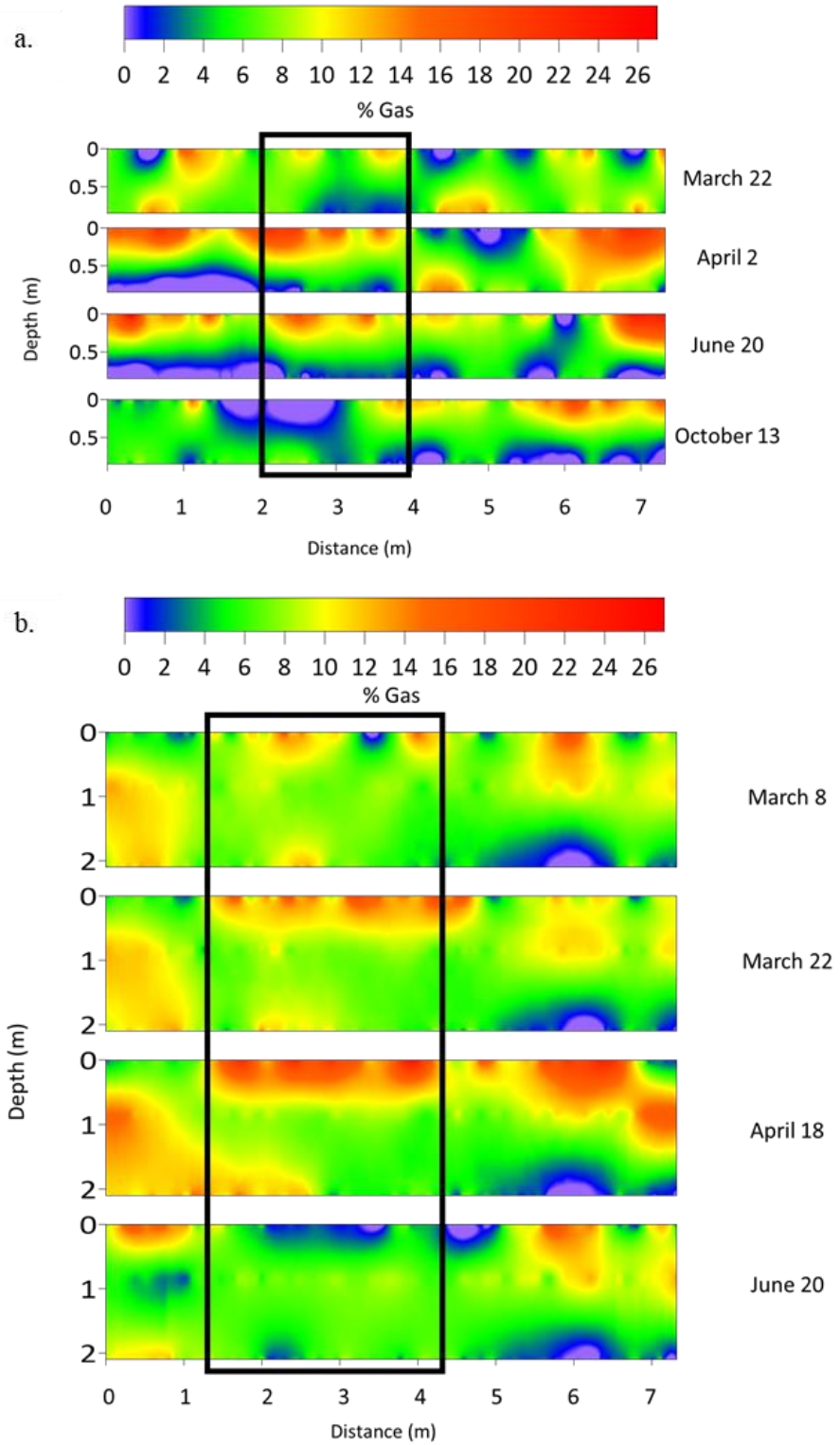

Figure 5. 2-D distribution of gas content from four separate days of the study in 2018 at Site E (a) and Site W (b). The black box is the area shown as a potential hotspot within the first layers of both sites.

4.3 GAS TRAP DATA

The volume of gas captured in the gas traps in between measurements was used to infer: 1) gas fluxes; and 2) gas composition in terms of methane and carbon dioxide. Gas composition from volumes collected from gas traps at Site E ranged from 10.9-55.0% CH_4 for the duration of the experiment, with an average of 31.9%. Site W ranged from 1.1-41.0% CH_4 with an average of 20.2%. Using this information, methane gas fluxes are calculated and displayed in Figure 6, and show consistent values when comparing the two sites, i.e. Site E and Site W in Figure 6a and 6b respectively. For example, Site E ranged from 9.8-213.5 mg CH_4 m^{-2} d^{-1} (with an average of 83.1 mg CH_4 m^{-2} d^{-1}). While Site W ranged from 0.2-190.2 mg CH_4 m^{-2} d^{-1} (with an average of 47.9 mg CH_4 m^{-2} d^{-1}). Also, CH_4 flux from Site E was lowest on December 12, 2017 and peaked on June 6, 2018. Similarly, at Site W, flux was lowest on January 24, 2018 and peaked on June 20, 2018.

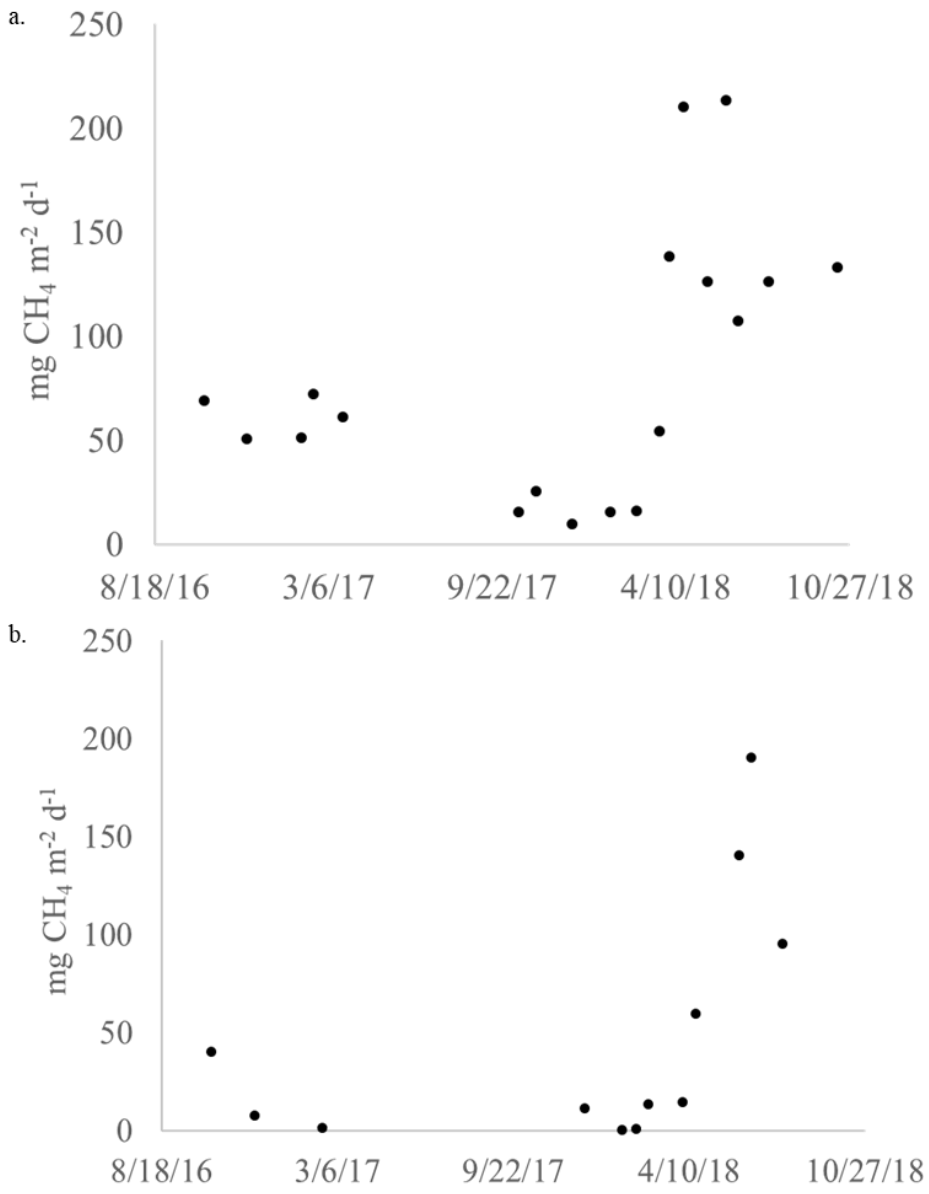

Figure 6. Methane flux values taken from gas traps at Site E (a) and Site W (b).

4.4 Correspondence of GPR data with gas traps

In order to further constrain our GPR datasets, average gas releases estimated from changes in GPR gas content in between measurements were compared with gas releases as inferred from the gas captured in the gas traps at Site E (Figure 7a) and Site W (Figure 7b) respectively. In both cases, a significant direct linear correlation ($P<0.05$)

exist between gas volumes collected in the gas traps and gas content release as inferred from the periods of gas content decrease in the GPR profiles.

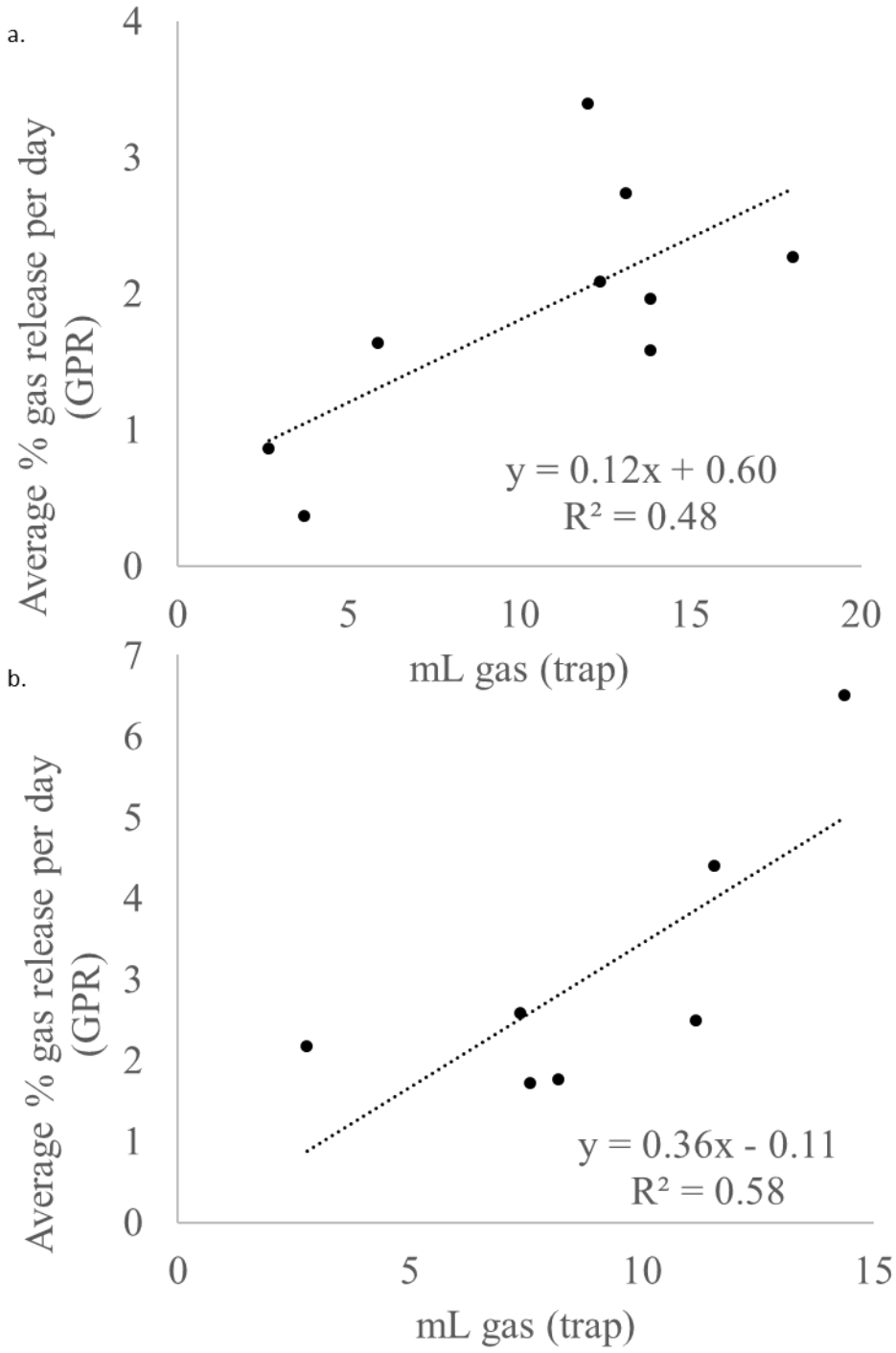

Figure 7. Gas trap and GPR comparison from methane flux values from Site E (a) and Site W (b). P-values for the sites were 0.039 and 0.047 respectively.

5 DISCUSSION

5.1 SPATIAL DISTRIBUTION OF HOTSPOTS FOR GAS CONTENT ACCUMULATION

One of the most striking results of this study is the spatial variability in gas content identified across the platforms. Despite the differences in thickness of the peat column between sites, results are consistent for both platforms and show: 1) the presence of specific areas within each platform characterized by consistent gas build-up and release over time, that we associate with hotspots (i.e. between 2-4 m distance along Site E, or 1.4-4 m distance along Site W, Figure 4); 2) the presence of areas within each platform where changes over time are insignificant (i.e. between 5-7 m distance along Site W, Figure 5); 3) the variability in gas content distribution with depth (i.e. layer distribution); and 4) gas content values that reach up to 28% at specific locations and are consistent with values from other studies in boreal peatlands describing areas up to 30% gas content [Comas et al., 2011; Parsekian et al., 2011]. At both sites, the largest gas contents recorded and the largest changes in gas content build-up and release correspond to the shallowest layer (i.e. L1E and L1W in Table 2, and Figure 4). Furthermore, inferred 2D images of gas content showed areas of increased activity (i.e. gas content build-up and release) with dimensions similar for both sites (i.e. with pockets ranging between 1-2 m wide and about 0.5 m tall), that were associated with hotspots. The dimensions of these hotspots fit within the limits of previous data from boreal peatlands [Comas et al., 2005; Parsekian et al., 2011], however they are about an order of

magnitude larger than previous laboratory data from the Everglades [Mustasaar and Comas, 2017]. The limitations in terms of sample size for that study however (about 0.5 m wide and 0.3 m tall) may be the cause of this discrepancy. Also, while the validity of the approach shown in this study has been already demonstrated in several other recent works, including the work in the Everglades referenced above, overall patterns of gas accumulation and release inferred from the GPR are consistent with patterns of release in the gas traps (Figure 7), confirming the validity of this approach.

We attribute the presence of these areas of increased accumulation and release of biogenic gases (or hotspots) to differences in the physical properties of the peat's matrix that may ultimately dictate the presence and activity of methanogens, based on the observed pattern where the areas of increased accumulation (i.e. the shallowest layer at each platform) coincide with the highest average porosity and lowest humification (von Post) values. We hypothesize that low humification increases the competency of the peat's matrix, increasing porosity thereby allowing gas to accumulate. Furthermore, substrate quality has been linked to decomposition as one of the main limiting factors influencing CH_4 and CO_2 production [Bridgham and Richardson, 1992; Reiche et al, 2010]. For that reason, it seems reasonable to expect higher gas production in those areas with lower humification (i.e. top layers L1E and L1W), and potentially higher substrate quality. This interpretation also coincides with some recent studies in peat soils from the Everglades where nearby sites from WCA-2 showed larger methane gas production rates associated with lower humification and higher porosity [Wright and Comas, 2016]. Other recent studies have also attributed the presence of hotpots for the accumulation and

release of biogenic gases in peat soils of the Everglades to contrasts in the physical properties of the soil matrix [Mustasaar and Comas, 2017; Wright et al, 2018].

5.2 TEMPORAL DISTRIBUTION OF HOTSPOTS AND GAS FLUX DYNAMICS

Contrasts in gas content are not only patent as lateral and vertical spatial variability within each platform interpreted as hotspots, but also as marked temporal variability along those same inferred hotspots, showing that changes in activity along these areas are consistent. Some of these trends can be followed in the time-lapse images in Figure 5. For example. the area highlighted in Figure 5a between 2-4 m distance along the platform shows what can be interpreted as vertical migration of gas with gas content decreasing in the bottom layer and shifting toward the top layer that shows an increase during March 22, April 2, and June 20 followed by a large decrease at the top layer during October 13. Similar trends can also be seen in other areas of Site E (i.e. 0-1 m or 6-7 m distance, Figure 5a), or similar size areas in Site W, i.e. increased gas accumulation and/or production between 1.5-4 m distance along the profile at the top layer during March 8, March 22, and April 18, followed by a large decrease during June 20. While not sequential in time, Figure 4 also depicts well how certain areas and layers along the profile show a lot of temporal variability (i.e. 1.5-4 m for L1W in Site W, Figure 4b), while others show almost no temporal variability (i.e. 3-6 m distance along the profile for L2W and L3W in Site W, Figure 4b).

Gas content variability observed along hotspots also provides information about flux dynamics at those particular locations and exemplifies the variability of flux values across the sites. For example, within the hotspot area comprised between 2.1-3.9 m along

the profile at Site E, layer L1E shows a gas build-up equivalent to 3,170 mg CH_4 m^{-2} d^{-1} between March 22-April 2, or a gas flux release of 160 and 1,990 mg CH_4 m^{-2} d^{-1} for the periods between April 2-June 20 and June 20-October 13 respectively. Similarly, within the hotspot area between 1.3-4.3 m along the profile at Site W, layer L1 shows a gas build-up equivalent to 507 and 387 mg CH_4 m^{-2} d^{-1} between March 8-March 22, and March 22-April 18 respectively, or a gas flux release of 906 mg CH_4 m^{-2} d^{-1} for the period between April 18-June 20.

5.3 RELATION BETWEEN SOIL'S PHYSICAL PROPERTIES AND GPR FACIES

Another interesting aspect of our datasets relate to the nature of the reflection record in the common offsets collected. The profiles suggest that differences in physical properties such as humification and porosity within the peat layers can alter the appearance of the GPR profile (i.e. GPR facies). For example, the discontinuous and chaotic configuration of reflectors of L1W at Site W (Figure 3b), coincides with the part of the peat column with lowest humification and largest porosity. Since that low humification implies the presence of clearly defined plant remains without any amorphous material that may act as point reflectors, it seems reasonable to expect the presence of numerous diffractions and more chaotic patterns. On the other hand, increased humification implies more pasty plant remains with no structure, and therefore less point reflectors that will result in a more horizontal and continuous distribution of reflectors for L2W and L3W, as shown in Figure 3b that may even show an increased signal attenuation as humification induces materials to become finer and pastier. A similar pattern can also be described for Site E, with the shallowest layer L1E also

showing a more chaotic pattern that extends to about 0.5-0.75 m coinciding with a lower humification, followed by a clearer pattern of laterally continuous and horizontal reflectors at L2E corresponding to a higher humification. It is also important to note that the large diffractions virtually extending the entire profile (and consecutively separated by about 2 m), correspond to wave reflections from the legs of the platforms, which extend from the surface to the mineral soil.

5.4 SITE COMPARISON AND SEASONAL GAS FLUX PATTERNS

The gas content, gas flux release, and gas build-up values shown in this study are well within the range of previous studies in the Everglades (i.e. Table 1). The range of methane flux values are also fairly similar when comparing the two investigated sites, however, overall values are slightly higher for Site E when compared to Site W (i.e. Figure 6a vs. 6b). It is interesting to note that while Site W is thicker than Site E (2.95 vs 1.9 m average), Site E shows overall larger average gas content (6.5 vs. 4.0 m at Site W) and larger maximum gas content as well (16.1 vs. 12.6 % gas content at Site W) (Table 2). While further analysis will be required to better understand the nature of this variability between sites, recent studies have shown that differences in the physical characteristics of the peat matrix may dictate differences in methane production in several sites in the Everglades (Wright and Comas, 2016). Considering the differences in physical properties between our two sites (i.e. particularly in terms of humification and porosity) it seems reasonable to anticipate differences in spatial and temporal distribution of biogenic gases between the two sites.

Overall gas flux trends for the two sites and for the entire period of data collection (extending for a total of 219 days) are also similar. As depicted in Figure 6, both sites show a methane flux increase of about one order of magnitude during the wet season (typically extending in Florida between mid-May through November), when compared to some of the measurements collected during the dry season (typically between December and mid-May). For example, the average CH_4 flux at Site E (Figure 6a) is 24.0 mg CH_4 m^{-2} d^{-1} between October 11, 2017 and February 23, 2018 while the average CH_4 flux between April 18 and July 25, 2018 is 153.7 mg CH_4 m^{-2} d^{-1}. Similarly, in Site W (Figure 6b), average flux between December 12, 2017 and April 2, 2018 is 6.6 mg CH_4 m^{-2} d^{-1} while average flux is 121.3 mg CH_4 m^{-2} d^{-1} between April 18 and July 25, 2018. These results are consistent with changes in water table elevation and temperature, which is a well-known factor to affect the releases of biogenic gas into the atmosphere [Daulat and Clymo, 1998; Glaser et al., 2004; Bon et al., 2014; Chen and Slater, 2015].

6 CONCLUSION

In this study we show the ability of GPR to non-invasively estimate the presence and dimensions of hotspots of biogenic gas from two sites within WCA-1 of the Florida Everglades. The GPR data is supported by other methods such as gas traps and time-lapse cameras. Both sites show areas of consistent gas buildup and release that are associated with hotspots that vary significantly over time. The largest average gas contents and largest overall gas contents were observed in the shallowest layers at both sites which we attribute to the peat's physical matrix. At both sites, the shallowest layers coincide with the lowest humification (von Post) values and the highest average porosity. The dimensions of the hotspots range from 1-2 m wide and approximately 0.5 m tall. Over time, these hotspots show high variations in CH_4 buildup and releases with buildups as high 3,170 mg CH_4 m^{-2} d^{-1} and releases as high as 1,990 mg CH_4 m^{-2} d^{-1}. Profiles from GPR suggest that the peat's physical structure can alter the appearance of the profiles as shown in the GPR profiles, with the lower humification and higher porosity areas are non-horizontal and more chaotic than the highly humified and lower porosity areas. Seasonal trends were also observed in gas releases that most likely correspond with changes in water table elevation and/or temperature as higher methane fluxes are observed during the wet season.

7 REFERENCES

American Society for Testing and Materials A. S. T. M. (2014), Standard test methods for moisture, ash, and organic matter of peat and other organic soils (D2974) edited, American Society for Testing and Materials, Philadelphia, 2014 Annual Book of ASTM Standards, doi:10.1520/D2974-14.

Baird, A. J., Beckwith, C. W., Waldron, S., & Waddington, J. M. (2004). Ebullition of methane-containing gas bubbles from near-surface Sphagnum peat. *Geophysical Research Letters*, *31*(21), doi:10.1029/2004GL021157.

Becker, T., Kutzbach, L., Forbrich, I., Schneider, J., Jager, D., Thees, B., & Wilmking, M. (2008). Do we miss the hot spots?? The use of very high resolution aerial photographs to quantify carbon fluxes in peatlands. *Biogeosciences Discussions*, *5*(2), 1097-1117, doi:10.5194/bg-5-1387-2008.

Bon, C. E., Reeve, A. S., Slater, L., & Comas, X. (2014). Using hydrologic measurements to investigate free-phase gas ebullition in a Maine peatland, USA. *Hydrology and Earth System Sciences*, *18*(3), 953-965, doi:10.5194/hess-18-953-2014.

Bridgham, S. D., & Richardson, C. J. (1992). Mechanisms controlling soil respiration (CO2 and CH4) in southern peatlands. *Soil Biology and Biochemistry*, *24*(11), 1089-1099, doi:10.1016/0038-0717(92)90058-6.

Červený, V., & Soares, J. E. P. (1992). Fresnel volume ray tracing. *Geophysics*, *57*(7), 902-915, doi:10.1190/1.1443303.

Chanton, J. P., Pauly, G. G., Martens, C. S., Blair, N. E., & Dacey, J. W. (1988). Carbon isotopic composition of methane in Florida Everglades soils and fractionation during its transport to the troposphere. *Global Biogeochemical Cycles*, *2*(3), 245-252, doi:10.1029/GB002i003p00245.

Chen, X., & Slater, L. (2015). Gas bubble transport and emissions for shallow peat from a northern peatland: The role of pressure changes and peat structure. *Water Resources Research*, *51*(1), 151-168, doi: 10.1002/2014WR016268.

Comas, X., Kettridge, N., Binley, A., Slater, L., Parsekian, A., Baird, A. J., Strack, M., & Waddington, J. M. (2014). The effect of peat structure on the spatial distribution of biogenic gases within bogs. *Hydrological processes*, *28*(22), 5483-5494, doi:10.1002/hyp.10056.

Comas, X., & Slater, L. (2004). Low-frequency electrical properties of peat. *Water Resources Research*, *40*(12), doi:10.1029/2004WR003534.

Comas, X., Slater, L., & Reeve, A. S. (2011). Pool patterning in a northern peatland: Geophysical evidence for the role of postglacial landforms. *Journal of hydrology*, *399*(3-4), 173-184, doi:10.1016/j.jhydrol.2010.12.031.

Comas, X., Slater, L., & Reeve, A. (2005). Spatial variability in biogenic gas accumulations in peat soils is revealed by ground penetrating radar (GPR). *Geophysical Research Letters*, *32*(8), doi:10.1029/2004GL022297.

Comas, X., Terry, N., Hribljan, J. A., Lilleskov, E. A., Suarez, E., Chimner, R. A., & Kolka, R. K. (2017). Estimating belowground carbon stocks in peatlands of the Ecuadorian páramo using ground-penetrating radar (GPR). *Journal of Geophysical Research: Biogeosciences*, *122*(2), 370-386, doi:10.1002/2016JG003550.

Comas, X., & Wright, W. (2012). Heterogeneity of biogenic gas ebullition in subtropical peat soils is revealed using time-lapse cameras. *Water Resources Research*, *48*(4), doi:10.1029/2011WR011654.

Comas, X., & Wright, W. (2014). Investigating carbon flux variability in subtropical peat soils of the Everglades using hydrogeophysical methods. *Journal of geophysical research: biogeosciences*, *119*(8), 1506-1519, doi:10.1002/2013JG002601.

Conrad, R., & Klose, M. (1999). Anaerobic conversion of carbon dioxide to methane, acetate and propionate on washed rice roots. *FEMS Microbiology Ecology*, *30*(2), 147-155, doi:10.1016/S0168-6496(99)00048-3.

Craft, C. B., & Richardson, C. J. (2008). Soil characteristics of the Everglades peatland. In *Everglades Experiments* (pp. 59-72). Springer, New York, NY, doi:10.1007/978-0-387-68923-4_3.

Daulat, W. E., & Clymo, R. S. (1998). Effects of temperature and watertable on the efflux of methane from peatland surface cores. *Atmospheric Environment*, *32*(19), 3207-3218, doi:10.1016/S1352-2310(98)00078-8.

Davis, S., & Ogden, J. C. (1994). *Everglades: the ecosystem and its restoration*. CRC Press.

Glaser, P. H., Volin, J. C., Givnish, T. J., Hansen, B., & Stricker, C. A. (2012). Carbon and sediment accumulation in the Everglades (USA) during the past 4000 years: Rates, drivers, and sources of error. *Journal of Geophysical Research: Biogeosciences*, *117*(G3), doi:10.1029/2011JG001821.

Gleason, P. J., & Stone, P. (1994). Age, origin, and landscape evolution of the Everglades peatland. *Everglades: the ecosystem and its restoration*, 149-197.

Green, S. M., & Baird, A. J. (2013). The importance of episodic ebullition methane losses from three peatland microhabitats: a controlled-environment study. *European journal of soil science*, *64*(1), 27-36, doi:10.1111/ejss.12015.

Huisman, J. A., Hubbard, S. S., Redman, J. D., & Annan, A. P. (2003). Measuring soil water content with ground penetrating radar. *Vadose zone journal*, *2*(4), 476-491, doi:10.2136/vzj2003.4760.

Joabsson, A., Christensen, T. R., & Wallén, B. (1999). Vascular plant controls on methane emissions from northern peatforming wetlands. *Trends in Ecology & Evolution*, *14*(10), 385-388 doi:10.1016/S0169-5347(99)01649-3.

Kellner, E., & Lundin, L. C. (2001). Calibration of time domain reflectometry for water content in peat soil. *Hydrology Research*, *32*(4-5), 315-332, doi:10.2166/nh.2001.0018.

Li, X., & Mitsch, W. J. (2016). Methane emissions from created and restored freshwater and brackish marshes in Southwest Florida, USA. *Ecological Engineering*, *91*, 529-536, doi:10.1016/j.ecoleng.2016.01.001.

Limpens, J., Berendse, F., Blodau, C., Canadell, J. G., Freeman, C., Holden, J., ... & Schaepman-Strub, G. (2008). Peatlands and the carbon cycle: from local processes to global implications-a synthesis. *Biogeosciences*, *5*, 1475-1491, doi:10.5194/bg-5-1475-2008.

McClellan, M., Comas, X., Benscoter, B., Hinkle, R., & Sumner, D. (2017). Estimating belowground carbon stocks in isolated wetlands of the Northern Everglades Watershed, central Florida, using ground penetrating radar and aerial imagery. *Journal of Geophysical Research: Biogeosciences*, *122*(11), 2804-2816 doi:10.1002/2016JG003573.

Mustasaar, M., & Comas, X. (2017). Spatiotemporal variability in biogenic gas dynamics in a subtropical peat soil at the laboratory scale is revealed using high-resolution ground-penetrating radar. *Journal of Geophysical Research: Biogeosciences*, *122*(9), 2219-2232, doi:10.1002/2016JG003714.

Myhre, G., Shindell, D., Bréon, F., Collins, W., Fuglestvedt, J., Huang, J., et al. (2013). Anthropogenic and natural radiative forcing climate change 2013: The physical science basis. In T. F. Stocker, D. Qin, G. K. Plattner, M. Tignor, & S. K. Al (Eds.), *Contribution of working group I to the fifth assessment report of the Intergovernmental Panel on Climate Change* (pp. 659–740). Cambridge and New York: Cambridge University Press.

Neal, A. (2004). Ground-penetrating radar and its use in sedimentology: principles, problems and progress. *Earth-science reviews*, *66*(3-4), 261-330 doi:10.1016/j.earscirev.2004.01.004.

Page, S. E., Rieley, J. O., & Banks, C. J. (2011). Global and regional importance of the tropical peatland carbon pool. *Global Change Biology*, *17*(2), 798-818, doi:10.1111/j.1365-2486.2010.02279.x.

Parish, F., Sirin, A., Charman, D., Joosten, H., Minayeva, T., Silvius, M., & Stringer, L. (2008). Assessment on Peatlands, Biodiversity, and Climate Change: Main Report, Global Environment Centre. *Wetlands International*, doi:10.1017/CBO9781107415324.004.

Parsekian, A. D., Comas, X., Slater, L., & Glaser, P. H. (2011). Geophysical evidence for the lateral distribution of free phase gas at the peat basin scale in a large northern peatland. *Journal of Geophysical Research: Biogeosciences*, *116*(G3), doi:10.1029/2010JG001543.

Reiche, M., Gleixner, G., & Küsel, K. (2010). Effect of peat quality on microbial greenhouse gas formation in an acidic fen. *Biogeosciences*, *7*(1), 187-198, doi:10.5194/bg-7-187-2010.

Richardson, C. (2008). *The Everglades experiments: lessons for ecosystem restoration*. Springer Science & Business Media.

Saragi-Sasmito, M. F., Murdiyarso, D., June, T., & Sasmito, S. D. (2018). Carbon stocks, emissions, and aboveground productivity in restored secondary tropical peat swamp forests. *Mitigation and Adaptation Strategies for Global Change*, *24*(4), 521-533, doi:10.1007/s11027-018-9793-0.

Shoemaker, W. B., Anderson, F., Barr, J. G., Graham, S. L., & Botkin, D. B. (2015). Carbon exchange between the atmosphere and subtropical forested cypress and pine wetlands. *Biogeosciences*, *12*(8), 2285-2300, doi:10.5194/bg-12-2285-2015.

Verry, E. S., Boelter, D. H., Päivänen, J., Nichols, D. S., Malterer, T., & Gafni, A. (2011). Physical properties of organic soils. *Peatland biogeochemistry and watershed hydrology at the Marcell Experimental Forest*, 135-176, doi:10.1201/b10708-6.

Waddington, J. M., Roulet, N. T., & Swanson, R. V. (1996). Water table control of CH4 emission enhancement by vascular plants in boreal peatlands. *Journal of Geophysical Research: Atmospheres*, *101*(D17), 22775-22785, doi:10.1029/96JD02014.

Warner, Barry G., David C. Nobes, and Brian D. Theimer. "An application of ground penetrating radar to peat stratigraphy of Ellice Swamp, southwestern Ontario." *Canadian Journal of Earth Sciences* 27.7 (1990): 932-938, doi:10.1139/e90-096.

Whalen, S. C. (2005). Biogeochemistry of methane exchange between natural wetlands and the atmosphere. *Environmental Engineering Science*, *22*(1), 73-94, doi:10.1089/ees.2005.22.73.

Wright, W., & Comas, X. (2016). Estimating methane gas production in peat soils of the Florida Everglades using hydrogeophysical methods. *Journal of Geophysical Research: Biogeosciences*, *121*(4), 1190-1202, doi:10.1002/2015JG003246.

Wright, W., Ramirez, J. A., & Comas, X. (2018). Methane ebullition from subtropical peat: testing an ebullition model reveals the importance of pore structure. *Geophysical Research Letters*, *45*(14), 6992-6999, doi:10.1029/2018GL077352.

Yu, Z., Loisel, J., Brosseau, D. P., Beilman, D. W., & Hunt, S. J. (2010). Global peatland dynamics since the Last Glacial Maximum. *Geophysical Research Letters*, *37*(13), doi:10.1029/2010GL043584.